MINERALOGICAL MAGAZINE, JUNE 1985, VOL. 49, PP. 457-467

The geochemistry of carbonate cements in the Avalon sand, Grand Banks of Newfoundland

IAN HUTCHEON,[1] CYNTHIA NAHNYBIDA,[1] AND H. R. KROUSE[2]

Sedimentology Research Group, Department of Geology and Geophysics,[1] and Department of Physics,[2] The University of Calgary, Calgary, Alberta, Canada T2N 1N4

ABSTRACT. Calcite cements from the Lower Cretaceous Avalon zone of the Hibernia field are, in places, extensively recrystallized, which complicates interpretation of the chemical and isotopic data. The oxygen isotopic data are widely scattered with $\delta^{18}O$ ranging between +1.6 and −9.2 for calcite and siderite. Siderite has lower $\delta^{13}C$ values (−6.6 to −13.2) than calcite +12.4 to −9.8. Typical trace element contents determined by ICP on acid-leached samples, range from 270 to 2100 ppm Sr and 180 to 2200 ppm Zn in calcite.

The trace element data indicate that some of the calcite has been precipitated from, or recrystallized by meteoric water. The trace elements show trends related to variations in $\delta^{18}O$ in such a way as to imply that not all the spread to low $\delta^{18}O$ values can be attributed to meteoric water influence alone. The data are not well enough constrained to calculate meaningful temperatures, but the range of $\delta^{18}O$ values probably represents an elevated range of temperatures of precipitation or recrystallization.

Microprobe analyses show that non-recrystallized fossils have a composition distinctly different from veins, cements, and recrystallized fossils, all of which are similar. The compositions of calcite cements are highly variable, with FeO (for example) ranging from 0.15 to 4.39 wt. %, but show no consistent patterns of zonation. Fossil fragments which show no textural evidence of recrystallization have low FeO contents (0.2 wt. %). Meteoric water, believed to be responsible for at least some of the cementation and recrystallization observed, probably entered the Avalon during and after formation of the mid-Cretaceous unconformity.

KEYWORDS: calcite, oxygen isotopes, carbonate cements, Avalon sand, Grand Banks, Newfoundland, Canada.

THERE are relatively few studies of diagenetic carbonate cements in siliciclastic rocks, even though carbonate cements are ubiquitous and second in abundance only to silica cements. Most published studies have focused on mudrocks (Irwin *et al.*, 1977) and the carbonates are generally interpreted as having formed very early, in the first few metres of burial. Studies of coarse-grained pore-filling cements in sandstones are less common, and the majority of these studies indicate that calcite cements formed before any significant compaction (Wright, 1964; Stalder, 1975). Some authors note the formation of carbonate cements at deeper levels of burial (Schmidt and McDonald, 1979; Nahnybida *et al.*, 1982) in sandstones and limestones.

In this study, carbonate cements in samples from the Avalon sand in the Hibernia field on the Grand Banks of Newfoundland (fig. 1) have been studied for their trace and major element content and isotopic composition. Petrography reveals many stages of cementation, some of which post-date compaction, and the objective of this study is to examine carbonate fossil fragments, recrystallization of these fragments, various carbonate cements and carbonate-filled veins, and relate them to the diagenetic history.

Geological setting. The Hibernia field is situated on a hinge zone within the Avalon Basin, which terminates against the Jeanne D'Arc Basin to the south. Benteau and Sheppard (1982) give an outline of the geology, the relevant features of which are summarized below. Fig. 2 shows an idealized cross-section of the Hibernia structure. Upper and Lower Cretaceous strata, separated by a mid-Cretaceous unconformity, overlie Jurassic and older rocks. There are large listric growth faults which cut the entire section down to, and in some cases including, basement. Some of these faults cut the mid-Cretaceous unconformity. Along the axis of the Avalon basin there are up to 15 000 m of sediment. To the south, in the Jeanne D'Arc Basin, Jurassic rocks subcrop against the mid-Cretaceous unconformity.

There are three major sand intervals in the Hibernia area. The Lower Cretaceous Avalon sand, which is the subject of this study, is the shallowest (2500 m) of the major reservoirs at Hibernia. There are carbonate cemented horizons within the Avalon zone which are laterally discontinuous and these cements are the focus of this paper.

Petrography. Carbonate in these samples occurs

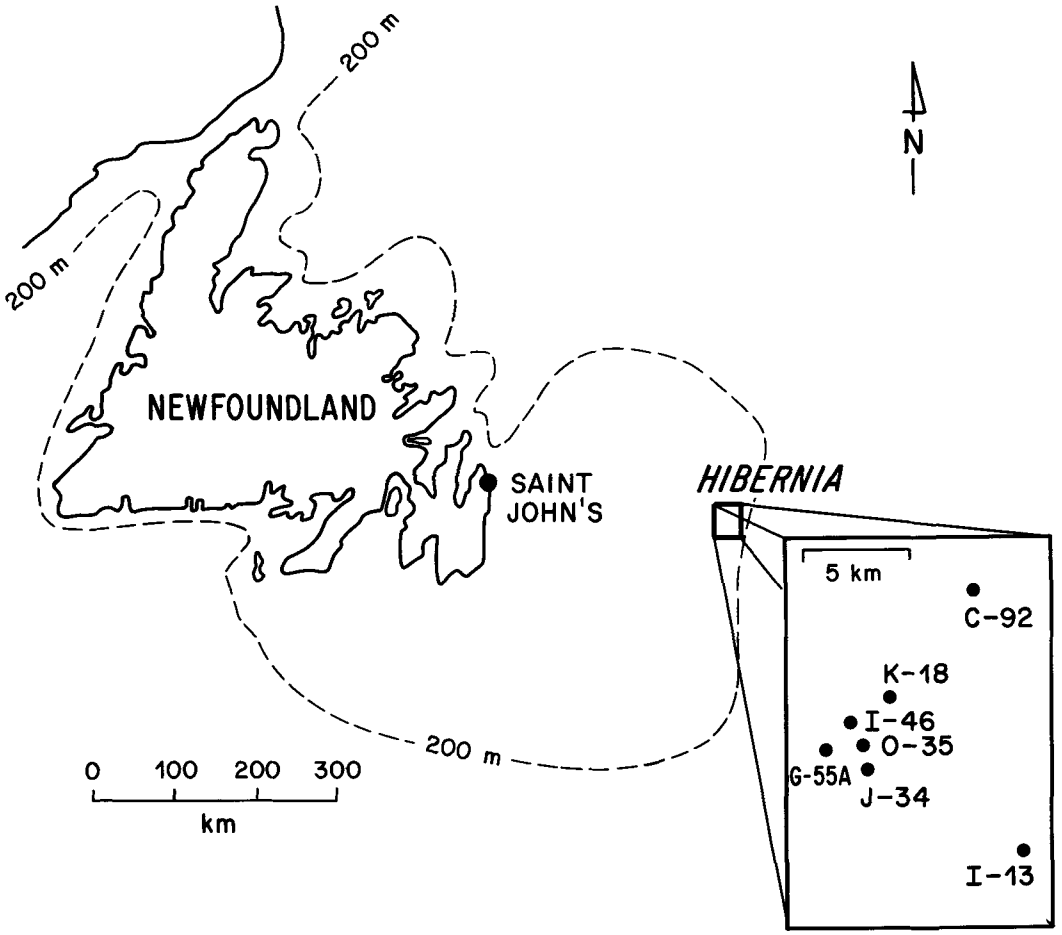

FIG. 1. Location map of the Hibernia field and the wells studied.

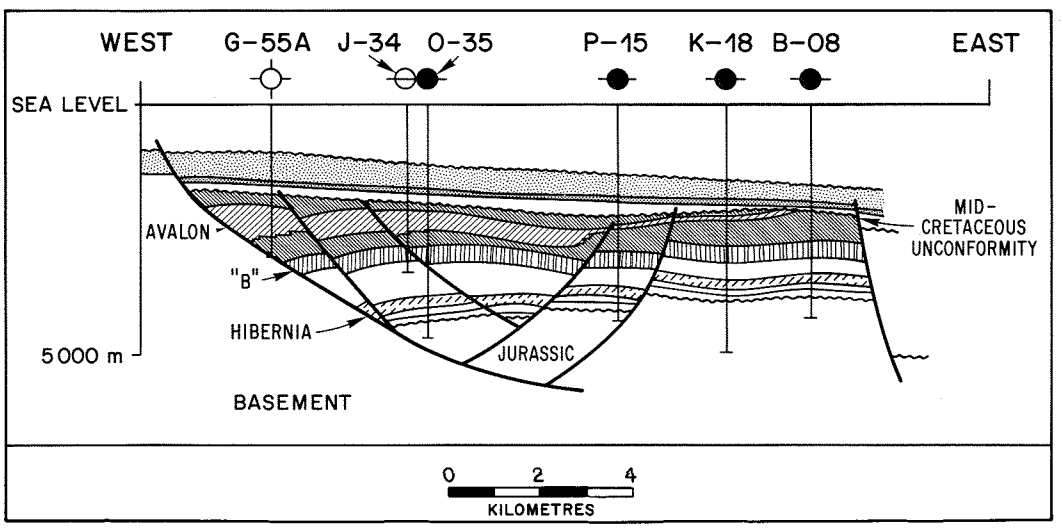

FIG. 2. An idealized cross-section of the Hibernia field showing the main Avalon, 'B' and Hibernia zones (after Benteau and Sheppard, 1982).

as bioclastic grains, grains of unknown origin, cements and veins. The textures observed in many samples indicate there has probably been extensive recrystallization of much of the carbonate in these rocks, making unequivocal interpretations of cement paragenesis difficult in some cases.

The texturally earliest cements observed include euhedral siderite grain-rimming cement (fig. 3*a*) and a calcite grain-rimming cement (fig. 4*d*) which is obscured by recrystallization in many places. The siderite cement forms very early in the diagenetic sequence and is observed within, and at the interface between, geopetal infillings of gastropod shells and pore-filling calcite cements.

Quartz overgrowths have been observed and predate at least some of the pore-filling cement. The quartz overgrowths are cut by calcite cement and represent either recycled quartz grains or replacement of quartz by calcite (fig. 3*b*). Interpenetrating quartz grains are not common. Some quartz grains are shattered (fig. 3*c*) and the fragments are enclosed by calcite cement. This would indicate that calcite cementation is relatively early, but occurred after sufficient burial, to cause shattering of quartz grains. The enclosing calcite cement is observed to be poikilotopic in many cases. A possible alternative interpretation is that the force of crystallization of the calcite caused grain breakage. Although the framework of the quartz grains appears to be open, with large calcite-filled pores, many of these 'open pores' on closer examination are actually recrystallized carbonate grains which were probably depositional in origin. In a few samples euhedral siderite can be observed rimming recrystallized grains

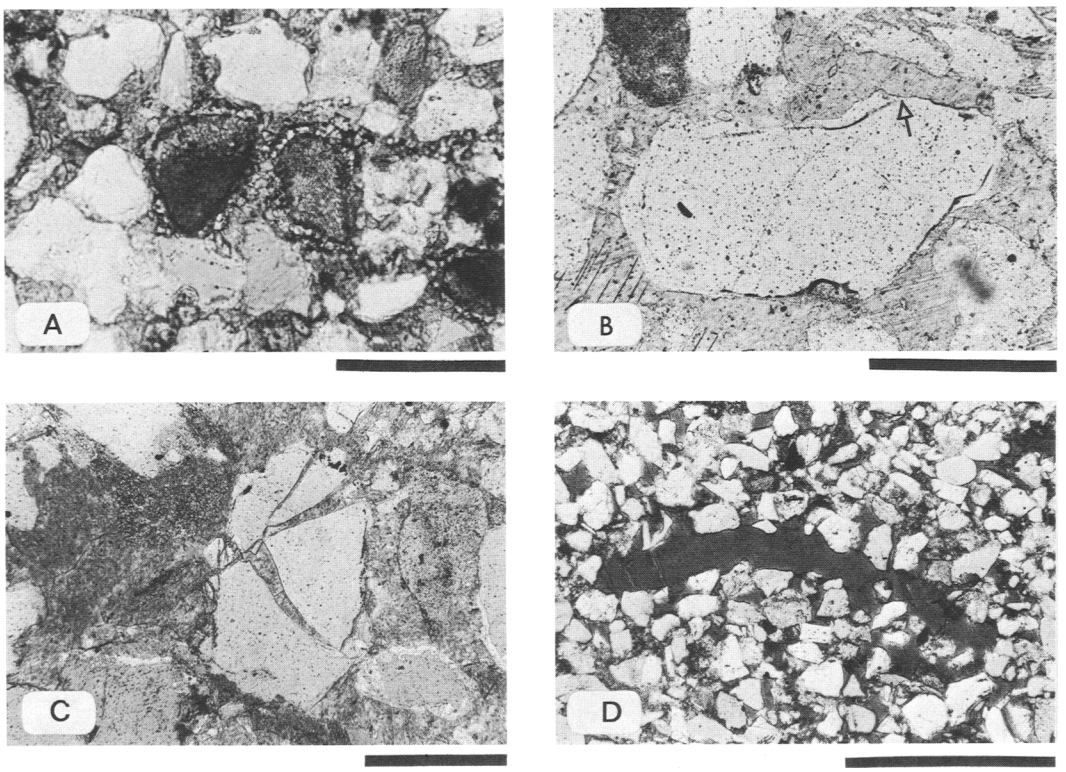

FIG. 3. (A) Siderite is present as an early, grain-rimming cement. Some calcite grains are recrystallized and appear to be pore-filling cement. The siderite rim on the calcite (which is stained and appears dark) permits recognition of the calcite as a detrital grain. Hibernia G-55A, 3353 m. Scale bar is 0.2 mm. (B) Although quartz overgrowths appear to predate calcite cement, the overgrowths are cross-cut (see arrow) by cement. Possible interpretations are either the quartz grain is recycled, or the calcite cement is replacing the quartz. Hibernia K-18, 3136 m. Scale bar is 0.25 mm. (C) Some quartz grains are shattered by calcite, and cemented so as to keep the fragments nearly in place. The calcite cement is poikilotopic. Hibernia K-18, 3136 m. Scale bar is 0.3 mm. (D) The latest stage of dissolution observed is that of pelecypod shells, often impinged by detrital quartz grains as a result of pressure solution. The calcite cement (stained and therefore dark) is poikilotopic and optically continuous with the shell fragment. Nautilus C-92. Scale bar is 1.0 mm.

which otherwise would appear to be pore-filling cement (fig. 3*a*).

The fossil fragments, which are abundant in some samples, show varying degrees of recrystallization, with gastropod shells showing the greatest tendancy to be recrystallized (fig. 4*a*) and pelecypod shells the least (fig. 3*d*). The 'pallisades' part of pelecypod shells are the most resistant to dissolution and are observed in many samples to be severely recrystallized and dissolved at contacts with quartz grains, as the only remaining fossil fragments (fig. 3*d*). Poikilotopic calcite cement is generally observed to be in optical continuity with fossil fragments. Some dissolution is very early. Fossil fragments are observed with dissolution pits which have subsequently been geopetally infilled with sand, calcite cemented and cut by veins (fig. 4*a*). Staining shows that, for samples with iron-calcite cements, recrystallized fossils and veins are also iron-rich. Some fossil fragments are only partly recrystallized, as is shown by staining.

While some of the cement is undoubtedly formed very early in the burial history, compaction and cross-cutting relationships indicate there must be a component of later precipitation of cement. Figs. 4*b* and *c* show serpulid worm tubes, with geopetal infill and cement. The tube in fig. 4*c* was cemented before compaction, while that shown in fig. 4*b* was cemented after some compaction. It is possible that the early rim cement (fig. 4*c*) may have protected some fossil fragments from crushing during the early stages of burial.

Point counts of the samples (fig. 5) show that there is a generally positive correlation between the percentage of bioclastic grains observed and the amount of cement. Some samples have cemented

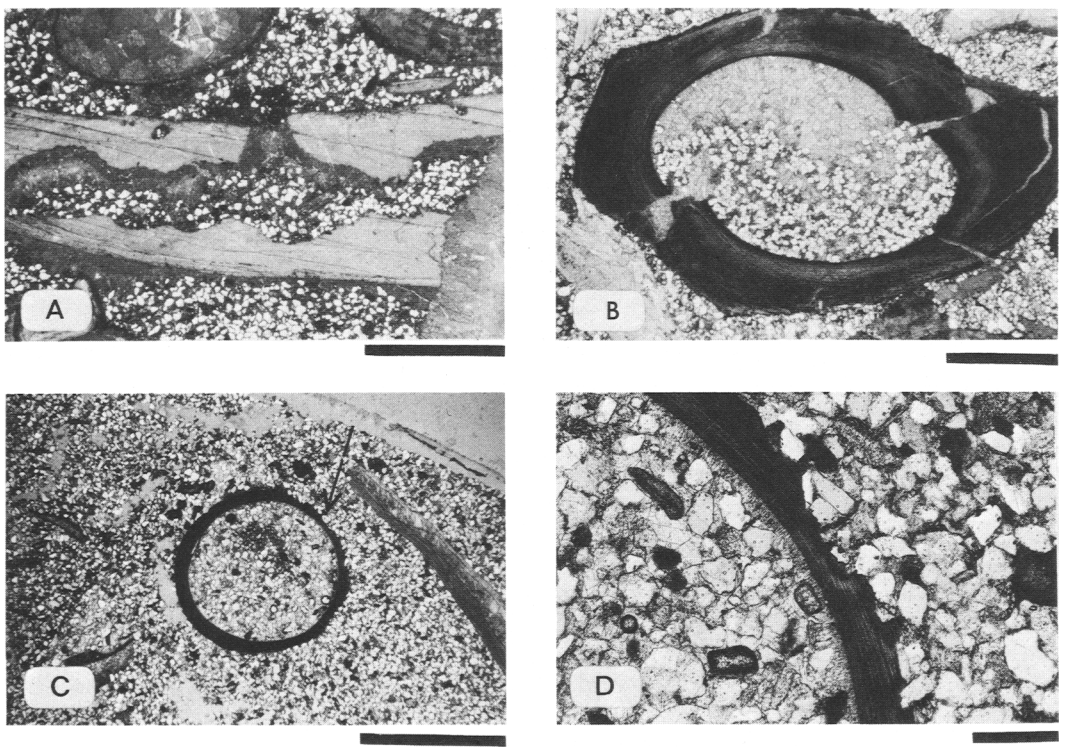

FIG. 4. (A) In this sample the pelecypod shell has been dissolved, geopetally infilled, a calcite rim cement has been deposited and this whole sequence is cut by an iron-rich calcite vein. The sample is stained and the non-recrystallized pelecypod shell appears lighter than the rim cement, vein, and the recrystallized fossil fragment in the upper left hand corner. Hibernia I-46, 2582 m. Scale bar is 2.0 mm. (B) Some geopetally filled fossil fragments show evidence of compaction before complete cementation of voids. Hibernia I-46, 2582 m. Scale bar is 1.0 mm. (C) This serpulid worm tube(?) shows little evidence of compaction. Arrow marks location of close up in (D). Hibernia I-13, 2735 m. Scale bar is 2.0 mm. (D) The rim of the worm tube(?) in 4(*c*) shows penetration by quartz grains, indicating possible pressure dissolution of the fossil fragments during burial. Note the well developed rim-cement on the inner surface of the spine. Hibernia I-46, 2582 m. Scale bar is 0.2 mm.

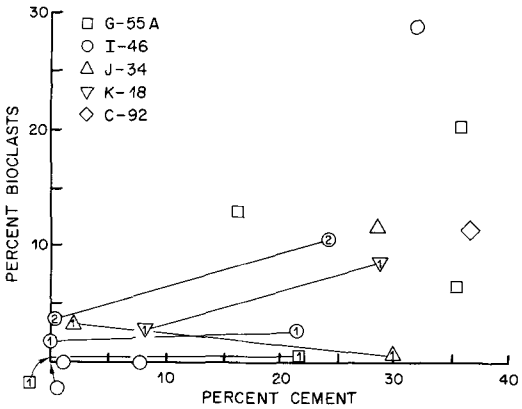

FIG. 5. Point counts for some of the samples show a general trend for samples with large amounts of bioclastic debris to have more cement. The symbols correspond to individual wells. Cemented and uncemented portions of the same sample were point counted separately and the number inside some symbols links cemented zones (high percent cement) and uncemented (lower amounts of cement) zones for a single sample.

and non-cemented portions. These samples tend to have relatively low amounts of bioclastic debris and the cemented samples in this group contribute significantly to the scatter observed in the data. Comparison of cemented and non-cemented areas of partially cemented samples shows that the non-cemented portions either show the same extent of compaction or are more severely compacted. This would imply that some of the cement probably post-dates compaction. It is not possible to use the textures to determine clearly when and in what relative amounts the cements formed.

Trace element compositions. The trace element composition of carbonates in 23 core samples was determined by crushing the rock and dissolving the carbonate in dilute HCl. The sample was dried and weighed before and after leaching. The acidic solution was made up to a known volume using double distilled water which was also used to wash the last traces of leachate from the crushed sample. This solution was then analysed by Induction Coupled Plasma (ICP) spectroscopy and the concentration of the water used with the weight measurements to calculate the trace element concentration in ppm for thirty elements. The ppm Ca was used to judge whether the majority of the dissolved constituents came from calcite dissolution, using the microprobe analyses to obtain the range of $CaCO_3$ contents of calcite. Only fifteen samples which apparently contained over 85 wt. % dissolved $CaCO_3$ in the solution (Table I) are used in interpretations of the data.

There are two major problems with this method. In the acidic solutions used, other minerals such as pyrite and chlorite are partially soluble and will contribute to the trace element composition as calculated for the carbonate. Minor amounts of Al were detected by ICP and it is likely that this results from dissolution of non-carbonates. Because the carbonates are, in the samples finally used in interpretation, volumetrically much more abundant than other soluble mineral phases, no correction was attempted. The second significant problem is that the various carbonate components of the rock are, in most samples, difficult, if not impossible, to physically separate in quantities sufficient for analysis. Because many of the carbonate components, particularly bioclastic fragments, show varying degrees of recrystallization, the problem of

Table I. Hibernia Calcite Cements - ICP Analysis (ppm)

WELL	S	Depth(m)	Cu	Zn	Co	Mn	Fe*	Sr	Cd	Mg*	Ba	Na	Ca*
G-55A		2447	77.03	203.49	29.07	1729.7	2.78	363.4	5.814	.261	4825.6	3813	47.1
		3353	1.54	19.29	3.86	1612.6	1.37	806.3	0.386	.042	19.29	1196	37.2**
	x	3367	7.83	6.91	2.30	1309.8	.101	435.1	0.691	.045	9.21	622	38.0**
I-46	x	2344	1.39	32.56	9.30	725.6	1.49	588.4	4.419	.113	16.28	1232	20.3
		2387	14.78	54.28	6.03	177.9	.311	974.1	2.110	.058	69.36	1206	32.4**
		2400	14.46	28.41	7.75	286.7	.314	271.2	0.517	.046	10.33	568	33.7**
	x	2457	7.53	43.01	5.38	521.5	.359	1354.8	2.688	.052	155.91	430	32.9**
		2498	22.43	32.56	3.52	428.2	.235	1081.8	1.809	.048	25.33	1013	35.8**
		2634	33.33	58.82	14.71	1205.9	.326	1357.9	0.980	.066	19.61	2598	31.4
O-35	x	2184	11.54	115.38	6.99	227.3	.500	1412.6	1.748	.057	38.46	1468	33.4**
K-18	x	2297	35.05	191.80	26.46	1216.9	.644	1567.5	4.630	.177	145.5	3968	30.2
		3132	5.68	23.24	2.58	2257.2	.229	960.7	0.258	.051	15.50	723	36.5**
		3136	21.20	25.32	3.16	1987.4	.215	1490.5	0.949	.042	12.66	443	37.1**
J-34	x	2458	14.00	275.95	20.59	1231.5	1.93	675.5	3.295	.168	28.83	3213	18.2
		2464	26.24	51.02	3.64	185.9	.358	1180.8	1.093	.046	25.51	1603	36.0**
		2483	24.55	41.49	3.46	190.2	.319	1030.4	1.037	.043	13.83	1141	35.1**
C-92	x	3331	44.55	130.84	10.61	834.5	.373	1326.0	0.354	.082	24.75	1273	33.5**
I-13	x	1892	9.62	84.13	4.81	324.5	.193	444.7	0.481	.886	16.83	721	36.7**
		1894	13.74	43.17	3.92	447.4	.181	2127.1	1.177	.030	2355	1295	37.2**
		2724	6.94	42.44	7.716	1747.7	.500	655.9	0.772	.125	111.88	1273	32.8**
		2735	8.00	138.59	31.98	1577.8	.569	3102.4	1.066	.215	117.27	3731	28.8

* Fe, Mg and Ca are given as wt. percent
** sample used for interpretation, Ca content indicates calcite as main dissolved component.
S siderite-bearing samples (x)
All wells are Hibernia, except C-92 (Nautilus) and I-13 (Hebron)

separating carbonate components is compounded. The acid soluble components of the 15 samples, which were deemed to represent calcite compositions accurately, are dominated by calcium carbonate and the values shown in fig. 6, which are an average of these samples, are believed to be representative. High Ca values reflect dissolution of anhydrite which is present as a vein filling. These analyses were not used for interpretation.

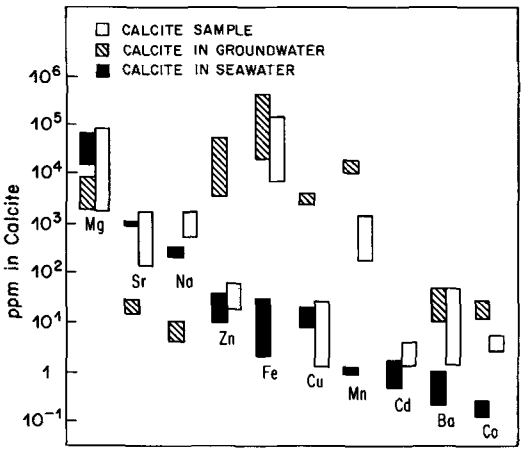

FIG. 6. The range of trace element values for the carbonates soluble in HCl (dominantly calcite) falls between equilibrium values for calcite in equilibrium with seawater and 'average' groundwater. (Ranges for seawater and groundwater calcite for all elements except for Ba from Veizer, 1983. Data for Ba from Drever, 1982; Kitano *et al.*, 1971). No distribution coefficient was available for Cd.

Shown on fig. 6 are the compositions of calcite in equilibrium with seawater and ground water. From the form of the distribution coefficient expression (Kinsman, 1969) it is clear that the important variable controlling the trace element concentration in calcium carbonate during a solution–reprecipitation process, like recrystallization, is the molar ratio in solution of the trace element to Ca. To calculate the equilibrium trace element compositions of carbonates, distribution coefficients were taken from White (1978), Richter and Füchtbauer (1978), Lorens (1981) and Viezer (1983). The ranges of trace element composition for calcite in equilibrium with seawater were taken from Viezer (1983) and the trace metal to Ca ratios for various elements in 'average' groundwater or meteoric water were obtained from the data of Majid (cited in Viezer, 1983) and Drever (1982). In the studied samples the trace elements Mg, Sr, Zn, Cu, and Cd have ranges which coincide, in part, with seawater, although the range may be much larger and extends to compositions which reflect groundwater. The trace element composition for calcite in equilibrium with groundwater generally coincides with some of the trace element content (Mg, Sr) or brackets the measured values (Fe, Mn) for the calcite in these samples. Only Na shows measured values completely at odds with the calculated values. This may result from saline groundwaters being produced by the dissolution of salts observed in the section (Benteau and Sheppard, 1982), or from the presence of numerous, small NaCl-bearing fluid inclusions. The cements were examined, unsuccessfully, for two-phase fluid inclusions.

Plots of various trace element ratios, which are not presented here, tend to show that the calcites in siderite-bearing samples have higher Fe/Ca ratios than calcite from non-sideritic samples. These same trends are observed for other elements. Generally the Mn/Ca ratio is independent of the Fe/Ca ratio and the Sr/Ca ratio is independent of the Zn/Ca ratio. Sr is apparently concentrated in calcite in preference to siderite, while Zn is concentrated in siderite. The Sr contents of some calcite are very high (2200 ppm) indicating the possibility that some calcite originates by dissolution and reprecipitation of aragonite.

Electron microprobe analyses. An ARL SEMQ electron probe microanalyser with seven spectrometers was used to determine the Ca, Mg, Mn, Fe, Sr, and Na contents of individual components in the samples studied. In total over 1000 analyses were collected, but only averaged data for selected samples with relatively clear-cut petrographic relationships are reported here. Analyses were performed at 15 kV with a beam current of 0.15 μA, emission current 300 μA, beam diameter 5 μm and counting times of 20 seconds. These operating conditions were used to maximize count rates while minimizing the volatilization of carbonates and still maintaining a minimum usable beam diameter. Averaged analyses are reported in Table II.

Figs. 7, 8, and 9 show representative profiles of Fe, Sr, Mn, and Mg across, respectively, pore filling cement, recrystallized and non-recrystallized fossil fragments to cement, and fossils to carbonate-filled veins. The calcite cements do not show any obvious zoning patterns, either random or at pore rims. Because the calcite 'cements' may be, in part, recrystallized fossil fragments, it is difficult to determine the exact nature of the minor compositional variations observed in the cements.

Fig. 7 shows graphically, for a single sample, a conclusion based on numerous analyses of cements. Variations in composition within the cement were minor in a single sample and were not systematic.

Table II. Averaged Electron Microprobe Analyses of Carbonate Components in Selected Samples (Weight Percent)

WELL#	DEPTH	COMPONENT	CaO	SrO	NaO	MnO	FeO	MgO	CO_2	TOTAL
I-46	2293	PFC	52.55±0.49	BDL	BDL	0.06±.02	3.69±.20	0.45±.04	44.03±.36	100.78±0.84
		F	52.82±1.10	0.10±.03	0.10±.04	BDL	0.27±.32	0.35±.42	44.42±.49	101.09±1.12
		RF	53.72±0.75	BDL	BDL	BDL	2.75±.53	0.33±.07	44.24±.31	101.09±0.69
		V	53.51±1.00	BDL	BDL	0.06±.03	2.60±.23	0.29±.06	43.91±.79	100.37±1.80
I-46	2344	F	53.92±0.55	0.07±.04	BDL	BDL	1.70±.19	0.64±.12	44.08±.37	100.41±0.85
		SD	4.80±0.90	BDL	BDL	0.20±.02	53.88±1.56	3.76±.48	40.99±.33	103.62±0.51
I-46	2387	PFC	53.71±0.83	0.12±.05	BDL	BDL	1.98±.40	0.69±.14	44.17±.47	100.67±1.07
		F	56.34±1.18	0.10±.03	0.13±.10	BDL	0.33±.72	0.21±.21	44.70±.37	101.82±0.79
I-46	2400	PFC	51.91±7.32	BDL	BDL	BDL	2.69±2.84	0.40±.11	43.40±.72	98.42±7.82
I-46	2634	PFC	53.56±0.76	0.23±.10	BDL	0.18±.04	2.69±.21	0.67±.08	44.62±.66	101.96±1.52
		F	54.39±0.22	0.10±.03	0.23±.04	BDL	0.10±.20	0.59±.16	43.45±.22	98.86±0.51
		RF	53.47±0.35	0.20±.06	BDL	0.19±.03	2.48±.32	0.62±.11	44.36±.31	101.33±0.72
J-34	2458	PFC	50.95±2.12	0.06±.04	BDL	0.14±.06	4.39±1.19	0.79±.32	43.46±1.14	99.80±2.41
		F	55.72±1.42	0.16±.11	BDL	BDL	1.43±.99	0.33±.11	45.05±.56	102.73±1.09
G-55A	3353	PFC	53.72±0.83	0.13±.11	BDL	0.18±.06	1.38±.38	0.46±.14	43.68±.54	99.55±1.24
		V	54.42±0.84	BDL	BDL	0.17±.02	0.98±.18	0.43±.10	43.90±.65	99.92±1.47
G-55A	3367	PFC	55.45±0.74	BDL	BDL	0.13±.04	0.89±.22	0.32±.08	44.51±.57	101.35±1.30
		V	55.10±0.53	BDL	BDL	0.20±.06	0.73±.12	0.40±.16	44.26±.41	100.70±0.94
K-18	3136	PFC	53.19±1.45	0.20±.09	BDL	0.25±.05	2.20±.26	0.45±.07	43.82±1.18	100.13±2.54
		F	54.08±0.48	0.13±.04	0.15±.05	0.21±.24	0.18±.08	0.97±.12	43.81±0.20	99.53±0.44
		PFC	53.38±1.18	0.23±.07	BDL	BDL	2.40±.41	0.41±.06	43.91±0.84	100.33±1.89
		RF	56.21±0.10	0.11±.01	0.12±.06	BDL	BDL	0.64±.31	44.87±0.27	101.97±0.54
		SD	6.19±0.31	BDL	BDL	0.21±.03	52.94±.55	3.83±.06	41.60±0.26	104.78±0.67
I-13	1892	PFC	53.70±1.26	BDL	BDL	BDL	1.94±.40	0.77±.19	44.19±0.92	100.64±2.09
		F	55.39±0.74	0.12±.03	.08±.04	BDL	0.25±.25	0.38±.24	44.09±0.35	100.31±0.80
		RF	53.66±1.03	BDL	BDL	BDL	2.03±.18	0.83±.13	44.28±0.68	100.83±1.56
		SD	5.56±0.15	BDL	BDL	0.45±.03	51.98±.35	3.52±.19	40.33±0.34	101.83±0.75
I-39	2724	PFC	53.48±.70	BDL	BDL	0.23±.13	1.53±.45	0.96±.23	44.13±0.52	100.37±1.20
		PFC	53.84±.92	0.14±.08	BDL	0.13±.06	1.49±.49	0.37±.24	43.71±0.63	99.70±1.39
		F	53.30±.75	0.11±.04	BDL	0.18±.07	1.63±.17	0.33±.07	43.33±0.57	98.87±1.31

ABBREVIATIONS:
PFC Pore filling calcite
F Fossil
RF *Recrystallized Fossil*
V Vein
SD Siderite
BDL Below detection limits

Very rarely some of the large cemented pores show calcite rimming the pore which is stained blue by ferricyanide, and a central red-stained pore filling. Analyses of these pores show minor, barely detectable variations in Fe content. In general, there is no change in Fe content for the pore filling cements within a single sample, although the cements do show very large ranges of composition between samples. This is in direct contrast to the late zoned carbonate cements in limestones noted by Wong and Oldershaw (1981).

Fig. 8 shows that fossil fragments (in this case a pelecypod shell) have low Fe and Mg contents and are higher (relative to the cement) in Sr and Mn than in portions which are not recrystallized. The recrystallized portions of fossil fragments have compositions which are more typical of the cements, especially where the cements have high Fe contents. This would indicate that the same fluids responsible for the most pervasive cementation also caused recrystallization of depositional carbonate components.

Fig. 9 shows a traverse across a vein which cuts through a bioclastic fragment which is not recrystallized. The veins are clearly enriched in Fe, Mn, and Mg and depleted in Sr, relative to the fossils. The veins show compositions which most closely resemble the cement, indicating that they may be related to cementation and recrystallization events. The minor element contents of the veins, cements and recrystallized fossil fragments tend to fall in a range between the composition of calcite in equilibrium with seawater or 'average' groundwater, generally closer to the groundwater equilibrium composition (fig. 6).

Isotopic data. The $\delta^{13}C$ and $\delta^{18}O$ composition of calcites were collected for samples from the Avalon sand (Table III). With difficulty, some fossil fragments and vein materials were separated. The isotopic composition of these components does not

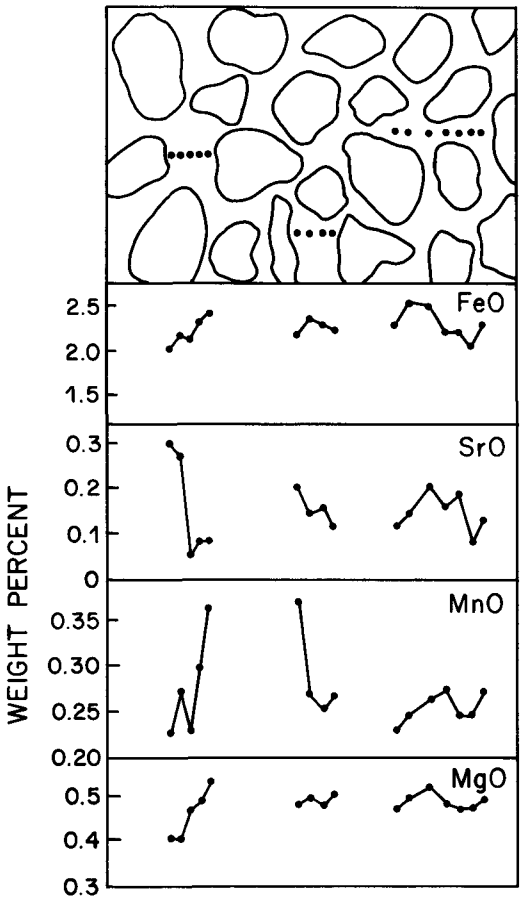

FIG. 7. Electron microprobe traverses across the pore-filling cements show little or no evidence of systematic zoning.

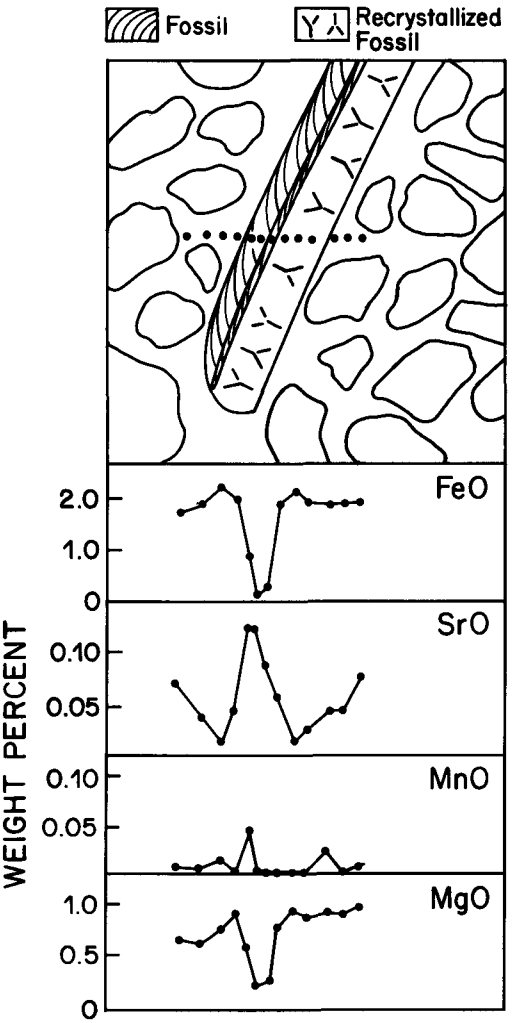

FIG. 8. Fossils which are not visibly recrystallized retain a composition which differs considerably from the cements. Recrystallized portions of fossils have compositions more typical of the cement.

show significant variations from the bulk value for the sample, probably because recrystallized fragments are difficult to identify; therefore no attempt was made to 'correct' the isotopic compositions on the basis of the point counts available for these samples. Physical separation, as done by Dickson and Coleman (1980), was not feasible for the samples available. Fig. 10 shows $\delta^{13}C$ plotted against $\delta^{18}O$ for calcite and, as might be expected for a system which displays variable degrees of recrystallization textures, there is considerable scatter in the data. The scatter of isotopic values is somewhat resolved if samples from the same wells are grouped together. If meteoric water has caused some of the recrystallization and cementation observed, this would indicate varying degrees of meteoric water input into different wells.

All stages of diagenesis of carbonate components, from processes which are probably early (siderite and calcite pore-linings) to later (recrystallization of fossil fragments and veining), are observed. As for the dolomites discussed in Irwin *et al.* (1977), some calcites are observed to have relatively heavy $\delta^{13}C$ with a considerable number of samples being close to the 0 per mil value. The samples are from a complex area with insufficient coverage to warrant detailed interpretation, but some features are worthy of note. Two samples, Hebron I-13 at 1894 m and Hibernia K-18 at 2297 m, show high,

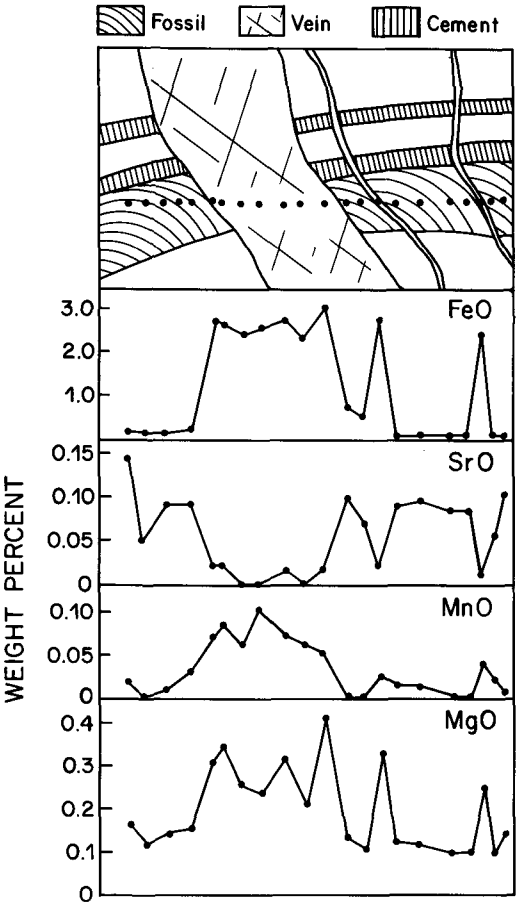

FIG. 9. Veins have compositions similar to the cements and, when in contact with fossil fragments, there is little evidence of compositional zoning in either the veins or the fossils.

positive $\delta^{13}C$ values (+12.4 and +7.0, respectively). A possible interpretation of these high $\delta^{13}C$ values is that they result from generation of methane. The methane removes the light $\delta^{13}C$ on evolution from the pore water and leaves the residual bicarbonate with heavier $\delta^{13}C$ which is then incorporated into the calcite cement. Very heavy $\delta^{13}C$ values are not commonly observed. Davies and Krouse (1975) report heavy $\delta^{13}C$ on samples from limestones. Further work by Beauchamp (pers. comm.) on samples from the same area studied by Davies and Krouse (op. cit.) suggests that methane generation within a relatively closed basin may be responsible for elevated $\delta^{13}C$ values within both depositional and authigenic carbonate components. Only authigenic components from Hibernia display heavy $\delta^{13}C$, suggesting that if generation of methane is responsible for the heavy $\delta^{13}C$ values, it occurred after some burial. Further sampling and analysis is required to resolve this problem.

TABLE III. Isotopic Compositions of Hibernia Calcite (C) and Siderite (S) Cements

Well	Mineral	S***	Depth(m)	δC^{13}	δO^{18}
Hibernia G-55A	CC		2447	-7.0	-9.8
G-55A	CC		2448	-8.3	-4.5
G-55A	CC		3353	-3.7	-6.1
G-55A	CC	x	3364	-4.1	-6.7
Hibernia I-46	CC		2293	-9.0	-1.9
I-46	CC	x	2344	+1.1	-5.2
I-46	SD		2344	-6.6	-1.9
I-46	CC		2387	+1.5	-5.0
I-46	CC		2400	0 -0.2	-0.9 -0.8
I-46	CC	x	2457	-2.1	-9.2
I-46	SD		2457	-10.8	+1.5
I-46	CC		2498	-0.2	-6.8
I-46	CC		2634	+0.1	-7.0
Hibernia O-35	CC	x	2184	+1.8	-5.7
Hibernia K-18	CC	x	2297	+7.0	-9.1
K-18	CC		3132	-5.4	-2.6
K-18	CC		3136	-0.7	-4.3
Hibernia J-34	CC	x	2458	-4.1	-4.0
J-34	SD		2486	-13.22	-0.74
J-34	CC		2464	+1.5	-7.2
J-34	CC		2483	+3.0	-7.1
J-34**A	CC	x	2551	-2.4	-6.0
J-34**B	CC	x	2551	-8.8	+1.6
Nautilus C-92	CC	x	3332	-1.8	-7.2
Hebron I-13	CC	x	1892	+0.7	-0.9
I-13	CC		1894	+12.4	-7.1
I-13	CC		2724	+1.0	-3.0
I-13	CC		2735	+0.4	-3.2

* All data relative to PDB standard.
**A = fracture fill
**B = cement
***S = ankerite or siderite-bearing samples (x)
CC = calcite
SD = siderite

By comparing trace element and isotopic data it may be possible to determine if the spread to more negative $\delta^{18}O$ is solely caused by meteoric water influence or if there is some effect of elevated temperature. Elevated temperatures would imply precipitation, or at least recrystallization, during later stages of burial. The ratios Sr/Ca and Mn/Ca show opposing trends when the compositions of calcites formed in meteoric water and marine water are compared. Generally, calcites formed in meteoric water will have lower Sr/Ca ratios and higher Mn/Ca ratios than their marine counterparts.

Some trends emerge if Sr/Ca and Mn/Ca are plotted against $\delta^{18}O$. Meteoric water should generally be depleted in $\delta^{18}O$ (more negative values) compared to marine water (Siegenthaler, 1979). Reported $\delta^{18}O$ values for groundwater range from −20 to −7 (Sklash and Farvolden, 1982; Fritz and Frape, 1982; Desaulnier *et al.*, 1982; Perry *et al.*, 1982). Calcites formed from meteoric water, at constant temperature, should show low Sr/Ca and high Mn/Ca values corresponding to more negative $\delta^{18}O$. If any trends are evident in

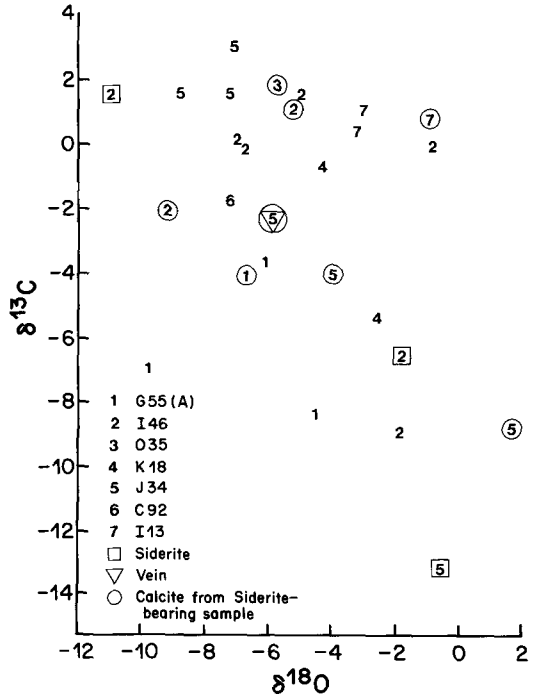

FIG. 10. Isotopic compositions of calcites and siderites. Individual wells are noted by numbers. The symbols indicate whether the analysis is of a siderite, calcite from a siderite-bearing sample or calcite. Trends in $\delta^{13}C$ and $\delta^{18}O$ are more evident if samples are separated by well location.

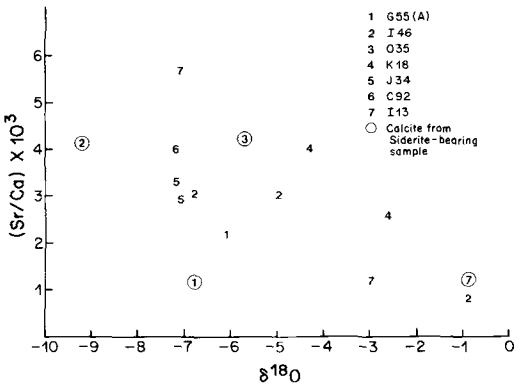

FIG. 11. The ratio of Sr/Ca for samples in which the major dissolved constituent is calcite tends to be low for more negative (lighter) values of $\delta^{13}O$. This is the reverse of the trend expected if $\delta^{13}O$ variations were due strictly to the input of metoric water.

plots of Sr/Ca *vs.* $\delta^{18}O$ (fig. 11) and Mn/Ca (fig. 12) *vs.* $\delta^{18}O$, they are the reverse of the expected trend. This would imply that there must be some effect of elevated temperature causing the depletion in $\delta^{18}O$. Since coexisting $\delta^{18}O$ values for groundwater are not known, temperatures cannot be calculated, but assuming values 2 per mil more negative than SMOW and using Craig (1965), temperatures up to 60 °C are calculated. Savin and Yeh (1981) show $\delta^{18}O$ values from -3 to $+3$ decreasing with depth, for pore waters squeezed from cores at several DSDP sites. Using their minimum value (-3) would decrease calculated temperatures somewhat.

Discussion and conclusions. Trace element data both from ICP and electron microprobe analyses, indicate an influence of meteoric water on the composition of some, if not all of the diagenetic calcite (cements, veins, and recrystallized bioclasts). Comparison of trace element and isotopic data indicate a possible effect of elevated temperature in the process of calcite precipitation and recrystallization. Temperatures estimated from isotopic compositions support the probability that the diagenetic calcite formed at some burial depth sufficient to elevate temperatures from surface values. The sequence in which the Avalon zone is found is most likely marine and possibly marginal marine. While definitive estimates of water depth at the time of deposition are not available, there is no compelling evidence to suggest that meteoric water invaded the Avalon very early in its burial history and that all the cements are therefore formed in the first few metres of burial. Some compaction features are observed in the cemented zones (e.g. fractured quartz grains healed by calcite cement, deformed

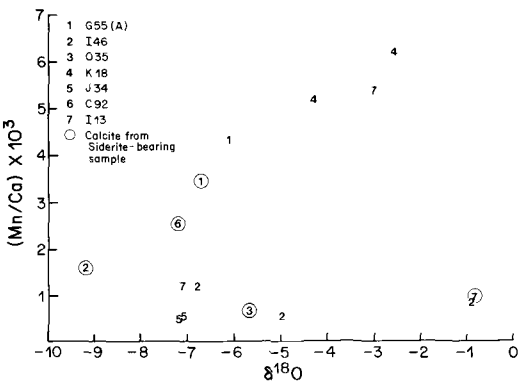

FIG. 12. The ratio of Mn/Ca for samples in which the major dissolved constituent is calcite tends to be high for more negative (lighter) values of $\delta^{13}O$. This is the reverse of the trend expected if $\delta^{13}O$ variations were due strictly to the input of meteoric water.

geopetally in-filled fossil fragments) indicating that at least some calcite cement must have been deposited at greater burial depths.

Biostratigraphic evidence (Thompson, Mobil Canada, pers. comm.) suggests that the mid-Cretaceous unconformity, which lies about 50–100 m above the Avalon zone, appears to represent a period of time ranging from 2 to 7 Ma. This is ample time, at that burial depth, for circulation of meteoric water into the Avalon zone. Above the unconformity there are about 100 m of fine grained clastic material with abundant, large shell fragments. This, combined with the bioclastic debris in the Avalon is a sufficient source for $CaCO_3$. In the mid-Cretaceous there was significant tectonic activity, faulting in the basin and rapid burial of the Avalon and the overlying bioclastic units to a depth of 400–600 m. This increase in burial depth, coupled with the influx of meteoric water, either along growth faults or directly into the Avalon, is probably responsible for the cementation and recrystallization observed.

In summary, the siderite cements observed formed at an early stage of burial. Considerable bioclastic debris was deposited with and above the Avalon sands and retains some of its minor element and isotopic signature as marine carbonate. This material served as the most immediate source of calcite cements but it is clear that, because of pervasive recrystallization, some calcite grains have been recrystallized and now appear to be 'cement' filling oversized pores. Some cement was derived from bioclastic debris by pressure solution of resistant quartz grains penetrating bioclastic fragments and probably from debris in overlying units. Elevated isotopic temperatures would support this conclusion. A major component of cementation, probably originating from the recrystallization of pre-existing carbonate, occurred during the time at which the mid-Cretaceous unconformity developed and allowed the influx of meteoric water into the Avalon sand.

Acknowledgements. This study benefited greatly from the co-operation and input of employees of Mobil Oil Canada, Ltd. J. Van Elsberg originally suggested the project and supplied lively discussion throughout and a thorough reading of previous versions of this manuscript. C. Chaplin provided much discussion of thin section textures and made available point counts of some samples. R. Gourlay helped provide a geological context and cleared many logistic barriers. L. Thompson offered advice and information on the biostratigraphy. We are also grateful to Mobil Oil Canada, Ltd. for access to their core storage facilities, the assistance of D. Blair and J. Broadfield, and permission to publish the results of this study. NSERC grants (IEH, HRK) and Mobil Oil Canada, Ltd. provided financial support.

REFERENCES

Benteau, R. I., and Sheppard, M. G. (1982) *J. Can. Petrol. Tech.* Nov.–Dec. 59–72.

Craig, H. (1965) In *Stable Isotopes in Oceanographic Studies and Paleotemperatures* (E. Tongiorgi, ed.). Cons. Nazionale delle Richerche, Labo. de Geologia Nucleare, Pisa, 161–82.

Davies, G. R., and Krouse, H. R. (1975) *Can. Geol. Surv. Paper* 75-1, part B, 215–20.

Desaulnier, D. E., Cherry, J. A., and Fritz, P. (1982) In *Isotope Studies of Hydrologic Processes* (E. C. Perry, Jr. and C. W. Montgomery, eds.), 45–55.

Dickson, J. A. D., and Coleman, M. L. (1980) *Sedimentology*, **27**, 107–18.

Drever, J. I. (1982) *The geochemistry of natural waters.* Prentice Hall, Englewood Cliffs, N.J., 388.

Fritz, P., and Frape, S. K. (1982) In *Isotope Studies of Hydrologic Processes* (E. C. Perry, Jr. and C. W. Montgomery, eds.), 57–63.

Irwin, H., Curtis, C., and Coleman, M. (1977) *Nature*, **269**, 209–13.

Kinsman, D. J. J. (1969) *J. Sed. Petrol.* **39**, 486–508.

Kitano, Y., Kanamori, N., and Oomori, T. (1971) *Geochim. J.* **4**, 183–206.

Lorens, R. B. (1981) *Geochim. Cosmochim. Acta*, **45**, 553–61.

Nahnybida, C., Hutcheon, I., and Kirker, J. (1982) *Can. Mineral.* **20**, 129–40.

Perry, E. C., Jr., Grundle, T., and Gilkeson, R. H. (1982) In *Isotope Studies of Hydrologic Processes* (E. C. Perry, Jr. and C. W. Montgomery, eds.), 35–43.

Richter, D. K., and Füchtbauer, H. (1978) *Sedimentology*, **25**, 843–60.

Savin, S. M., and Yeh, H. W. (1981) In *The Sea*, **7**, *The Oceanic Lithosphere* (C. Emiliani, ed.), Wiley-Interscience, 1521–54.

Schmidt, V., and McDonald, D. A. (1979) In *Aspects of Diagenesis* (P. A. Scholle and P. R. Schluger, eds.). SEPM Spec. Publ. **26**, 175–208.

Siegenthaler, U. (1979) In *Lectures in Isotope Geology* (E. Jäger and J. C. Hunziker, eds.), 264–73.

Sklash, M. G., and Farvolden, R. N. (1982) In *Isotope Studies of Hydrologic Processes* (E. C. Perry, Jr. and C. W. Montgomery, eds.), 65–73.

Stalder, P. J. (1975) *Geol. en Mijnbouw*, **54**, 148–56.

Viezer, J. (1983) *SEPM Short Course*, **10**, Dallas, 1983.

White, A. F. (1978) *Chem. Geol.* **26**, 65–72.

Wong, P., and Oldershaw, A. (1981) *J. Sed. Petrol.* **51**, 507–20.

Wright, M. D. (1964) Ibid. **34**, 756–60.

[*Manuscript received 14 April 1984; revised 28 August 1984*]